Pharmaceutical Research, Vol. 26, No. 3, March 2009 (© 2009)
DOI: 10.1007/s11095-008-9813-y

Research Paper

Novel Pentablock Copolymers for Selective Gene Delivery to Cancer Cells

Bingqi Zhang,[1] Mathumai Kanapathipillai,[1] Paul Bisso,[2] and Surya Mallapragada[1,3]

Received September 5, 2008; accepted December 15, 2008; published online January 14, 2009

Purpose. In this study, the novel poly(diethylaminoethylmethacrylate) (PDEAEM)/Pluronic F127 pentablock copolymers were found to be able to mediate high-efficiency transfection of human epithelial ovarian carcinoma (SKOV3) cell line while showing significantly lower efficacy in human epithelial retinal (ARPE-19) cell line and Swiss Mouse Fibroblast (3T3) cell line.
Methods. The intracellular routes of polyplexes were investigated by confocal microscopy after appropriately labeling the polymer and DNA.
Results. It was found that lesser nuclear entry in the ARPE-19 cells may result in the lower efficiency of transfection. Since the SKOV3 proliferation rate was found to be much higher than that of the ARPE-19 cells, the nuclear entry of polyplexes was assumed to be correlated with the proliferation rate, and it was hypothesized that the novel pentablock copolymers could mediate gene delivery selectively in fast growing cells. The different intracellular barriers to gene transfer may also account for the observed difference of transfection efficacy.
Conclusions. Although the validity of the hypothesis that our pentablock copolymer could selectively transfect hyperproliferative cells needs further examination, this present work provides a new perspective to design targeting vectors for cancer therapies based on different characteristics among specific cell types.

KEY WORDS: confocal microscopy; gene therapy; intracellular trafficking; non-viral gene delivery; targeting.

INTRODUCTION

One of the features of the ideal non-viral transgene vector is cell specificity, which is so far usually achieved via receptor-mediated endocytosis by integrating cell specific ligands in the gene transfer system (1–3). With a receptor on the target cell surface and a matching ligand that can be attached to the synthetic vector, a targeting gene delivery system could be established and expected to enhance the gene expression by increasing cellular uptake in the specific cell types. Through this receptor-mediated uptake, only the cells having some recognized over-expressed receptors could be "designed" as the target with the prerequisite that the ligand is also available and attachable to the vector of interest without compromising its DNA condensing ability, serum resistance and/or other particular properties. Commonly investigated ligands include asialoglycoprotein specific for hepatocytes (4–6), mannose for macrophages (7–9), and transferrin (10,11)and folate (12,13) for certain tumor cells. These have been reported to improve the transfection efficacy selectively in the target cells. Although the polymeric vectors have great flexibility to be tailored for particular applications like ligand modification, there are several limitations of this approach. In many cases, the receptors are over-expressed on the specific cell types, but they are also expressed by other cells, thereby decreasing the targeting efficiency. Moreover, interactions with serum proteins in the bloodstream and aggregation could further reduce the specificity of cellular uptake (14,15). A well known fact is that the same gene delivery system may exhibit quite different transfection efficiencies in different cell types (16–18), indicating there are particular cellular characteristics that affect the gene expression and could potentially be used to build up a cellular screen to selectively express foreign genes by specific cells. As an important cellular characteristic, the cell cycle has been reported to play a significant role in gene transfer due to high dependence of gene expression on the mitotic phase, especially with the use of non-viral vectors (19–21). This suggests that the entry of complexes into the nucleus may require or benefit from the disruption of nuclear membrane; thus, the greater the number of cells entering mitosis, the higher the gene expression (19). But in some cases, mitotic activity would not act as a limiting factor if the vectors possess an excellent nuclear localization ability and

Electronic supplementary material The online version of this article (doi:10.1007/s11095-008-9813-y) contains supplementary material, which is available to authorized users.

[1] Department of Chemical and Biological Engineering, Iowa State University, 3035 Sweeney Hall, Ames, Iowa 50014, USA.
[2] Department of Chemical Engineering, Columbia University, New York, USA.
[3] To whom correspondence should be addressed. (e-mail: suryakm@iastate.edu)

turn out to be versatile like poly(ethyleneimine) (PEI) (22). However, if the vectors only have access to nucleus during mitosis, their transfection efficiency would be extremely dependent on how fast the cells proliferate. In other words, targeting could be achieved among cell types with significantly different proliferation rates, such as most tumor cells and normal cells, even without the use of targeting ligands.

In this present work, we report a novel pentablock copolymer with the potential selectivity to selectively transfect fast growing cells. The novel amphiphilic pentablock copolymer developed in our laboratory exhibits temperature- and pH-induced micellization and gelation (23). The central triblock Pluronic F127 contributes to the temperature responsiveness and has been reported to be able to promote cellular entry (24). The end-blocks of poly(diethylaminoethyl methacrylate) (PDEAEM) are the essential functional cationic segments to complex with DNA and to provide pH buffering in the endosome with their protonatable tertiary amine groups (25). In order to improve the stability and reduce the cytotoxicity caused by the excess positive charges on the surface of copolymer/DNA polyplexes, free Pluronic F127 was added to the polymer–DNA complexes to shield these excess charges (26). Previous work has proved the high transfection efficiency of the pentablock copolymer and the stabilization effect induced by Pluronic F127 in serum supplemented medium in cancer cell lines. Furthermore, this transgene system is also injectable and can form thermoreversible gels *in vivo* for sustained release. Therefore, combining its potential selectivity for transfecting fast-growing cells, and its ability to be injected intra-tumorally to form gels for sustained gene delivery makes it promising as an ideal sustained and targeted transgene vector for cancer therapies.

MATERIALS AND METHODS

MATERIALS

The SKOV3 human ovarian carcinoma, ARPE-19 human retinal and cell lines were obtained from ATCC™ (Manassas, VA). The 3T3 Swiss mouse fibroblast cell line was kindly donated by Dr. Nilsen-Hamilton's Laboratory (ISU, Ames). Living Colors™ HT-1080 Retro DsRed-Express cell line, a clonal human fibrocarcinoma derived cell line that stably expresses DsRed-Express, was obtained from BD Biosciences-Clontech. Cell culture reagents including Dulbecco's Modified Eagle Medium (DMEM), heat inactivated fetal bovine serum (FBS), 0.25% trypsin–EDTA and Hank's buffered salt saline (HBSS) were purchased from Invitrogen (Carlsbad, CA) and the Dulbecco's MEM: Ham's Nutrient Mixture F-12, 1:1 Mix (DMEM/F-12) from ATCC (Manassas, VA). Luciferase assay system and passive lysis buffer (PLB) were purchased from Promega (Madison, WI). HEPES salt used to make Hepes buffer saline (HBS), Lactate dehydrogenase (LDH) kit, paraformaldehyde and Bromodeoxyuridine (Brdu) were obtained from Sigma (St Louis, MO). Alexa Fluor®647 carboxylic acid, succinimidyl ester (written as Alexa 647 henceforth), ethidium monoazide (EMA), 4′,6-diamidino-2-phenylindole (DAPI) dilactate and ProLong® Gold antifade reagent were also purchased from Invitrogen (Carlsbad, CA). ExGen 500® (written as ExGen henceforth) was purchased from Fermentas Life Sciences (Hanover, MD). DNase I was purchased from Ambion (Austin, TX). HiSpeed Plasmid Maxi Kit was obtained from Qiagen (Valencia, CA). Pluronic F127 [$(PEO)_{100}$-b-$(PPO)_{65}$-b-$(PEO)_{100}$], (where PEO represents poly(ethylene oxide) and PPO represents poly(propylene oxide)) micro pastille surfactant was donated by BASF (Florham Park, NJ) and used without further modification.

Pentablock Copolymer Synthesis and Attachment of Alexa Fluor 647

The pentablock copolymer $PDEAEM_{13}$-b-PEO_{100}-b-PPO_{65}-b-PEO_{100}-b-$PDEAEM_{13}$ used in the present work (Scheme 1) was synthesized via atom transfer radical polymerization (ATRP) as previously reported (23), with M_n=17,533 and M_w/M_n=1.14, as judged by ^{1}H NMR (in deuterated chloroform) and Gel Permeation Chromatography (GPC) (tetrahydrofuran mobile phase, poly(methylmethacrylate) calibration standards) respectively. In order to attach the fluorescent dye Alexa Fluor 647 for intracellular trafficking studies, this pentablock copolymer was amine functionalized by transforming the bromine group into azide and then further into triphenylphosphine and finally into the amine group after hydroxylation (see Supplementary Scheme 1). The transformation was confirmed by the presence and subsequent absence of a

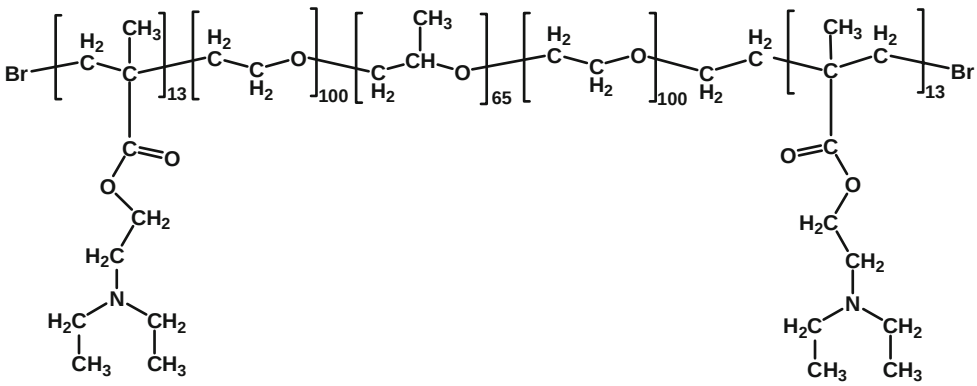

Scheme 1 Chemical structure of pentablock copolymers.

peak at about 31 ppm in the ^{31}P NMR spectrum. Alexa 647 was reacted with amine modified pentablock similar to a procedure reported previously (27). Briefly, for a 20 mg/ml polymer solution in 0.1 M sodium bicarbonate buffer, around 100 μg of the dye was added. The mixture was stirred in the dark at room temperature for 1 h. The unattached dye was removed by extensive dialysis for 2 days. The polymer with conjugated dye was then freeze dried.

Plasmid DNA Purification and EMA Attachment

Bacteria containing the 6.7 kb pGWIZ-luc plasmid (GeneTherapy Systems Inc, CA) encoding the luciferase reporter gene or the 4.7 kb pEGFP-N1 plasmid (ClonTech, CA) encoding for green fluorescence protein (GFP) were grown in selective Luria–Bertani (LB) medium and then purified using the Qiagen HiSpeed Maxi Kit. The concentration of DNA was tested using a NanoDrop spectrophotometer. A260/A280 was at least 1.8 for all DNA used. DNA was labeled with the fluorescent probe ethidium monoazide (EMA, 8-azido-3-amino-6-phenyl-5- ethylphenanthradinium chloride) according to the procedures reported elsewhere (28,29) with minor modifications. Briefly, appropriate amounts of plasmid and EMA were mixed giving a 50:1 molar ratio of nucleotide to probe. The solution was incubated on ice for 30 min before being exposed to UV light of principal wavelength 312 nm. After 20 min photolysis, most of the DNA had been covalently bound with EMA, and the excess EMA and intercalated EMA were removed by performing ethanol precipitation three times.

Polyplex Formation

Polymer/DNA polyplexes at various N/P ratios were formulated by adding appropriate quantities of unlabeled or labeled pentablock copolymer (2 mg/ml) solution in 0.5× HBS, pH 7.0 to plasmid DNA solutions which were properly prediluted with the same HBS buffer to get the equal mixing volume. The mixture was briefly vortexed and allowed to incubate at room temperature for 20 min to ensure complexation. If required, Pluronic F127 solution (10 mg/ml) in 0.5× HBS, pH 7.0 was added to the formulation to get the F127/pentablock copolymer wt. ratio of 5 with gentle vortexing followed by another 10 min incubation. We will be referring throughout this work to four abbreviations for the different vectors used to form polyplexes: P refers to the pentablock copolymer alone, Pd refers to the pentablock copolymer with the fluorescent dye attached, F refers to Pluronic F127, and correspondingly, P–F refers to the pentablock copolymer with subsequent added Pluronic F127 for shielding the excess positive charges.

Cell Culture

The SKOV3, 3T3 and HT1080 cells were grown in Dulbecco's Modified Eagles Medium (DMEM, Invitrogen) supplemented with 10% (*v*/*v*) fetal bovine serum (FBS, heat inactivated, GIBCO) at 37°C under a humidified atmosphere containing 5% CO_2. ARPE-19 cells were grown in DMEM/F-12 (ATCC) containing 10% FBS under the same conditions. Cells were passaged approximately every 2–3 days for SKOV3 and HT1080, 4–5 days for APRE-19 and 7–8 days for 3T3 cells.

In vitro Transfection

For the transfection based on luciferase activity, cells of interest were seeded into a 96-well plate at an initial density of 1.2×10^4 to 3×10^4 cells per well in 200 μl growth medium and allowed to incubate for 24–48 h depending on the cell type, to reach 70% confluence when transfection could be performed. Polyplexes prepared at given N/P ratios were added to the newly changed FBS-supplemented medium with 0.6 μg of DNA per well. After 3 h transfection at 37°C, the medium containing polyplexes was replaced with fresh growth medium and cells were allowed to grow for another 45 h post-transfection until the luciferase assay was performed. The total duration of transfection and post-transfection was kept at 48 h. ExGen 500, a sterile solution of linear 22 kDa polyethylenimine (PEI), was used as positive control at N/P ratio of 6 according to the manufacturer's protocol. The luminescence from lysed cells in 20 μl passive lysis buffer per well was measured in arbitrary Relative Luminescence Units (RLU) on an automated Veritas™ Microplate Luminometer using the Renilla Luciferase Assay System from Promega. Each transfection was done in triplicate.

To compare the transfection efficacy between different cell types, luciferase activity in each well was normalized by the total amount of proteins determined by Bicinchoninic Acid (BCA) protein assay kit and expressed as mean RLU per milligram of cell protein. As for the comparison between different conditions of the same type of cells, RLU per well was utilized to obtain values since transfection was performed with the same initial number of cells per well. In the trafficking experiments, cells of interest were seeded onto poly-L-lysine coated coverslips in six well-plates at a density of 1×10^5 cells per well and subsequently transfected with polyplexes at 3 μg DNA per well following the same procedures used in the case of 96-well plate. At specific time points during transfection or post-transfection, cells were fixed with 4% paraformaldehyde and mounted on the glass slide that held a drop of mounting medium to keep cells from drying out.

Specifically for the transfection of HT1080/ARPE-19 co-cultured cells, separately cultured HT1080 and ARPE-19 cells were seeded together onto six-well plates at varied ratios of cell number and incubated in co-culture media, 50/50 (*v*/*v*) until being transfected with polyplexes at 2 μg EGFP-N1 plasmid per well. EGFP expression was examined qualitatively by fluorescence microscopy and quantitatively by flow cytometry.

Flow Cytometry

After transfection, the cells were harvested from six-well plates and cells from each well were suspended in 3 ml HBSS. Then cell suspensions were transferred to 15 ml centrifuge tubes and centrifuged for 12 min at 1,200 rpm. Supernatants were removed and cells pellets were resuspended in 3 ml fresh HBSS. After another centrifugation, cells were finally suspended in 0.5 ml of 2% paraformaldehyde in PBS and stored at 4°C for later analysis with a Becton-Dickinson FACSCanto flow cytometer.

Cytotoxicity

The cytotoxicity of polyplexes was measured with LDH assay, as the amount of LDH in the cell culture medium is representative of the cell death following the membrane rupture. To get a better knowledge of the stage at which most cell death occurs, the LDH activity was assayed twice, at the end of 3 h transfection and after the additional 45 h post-transfection. Triton-X was used as a negative control to provide 100% cytotoxicity.

Confocal Microscopy

EMA and Alexa Fluor 647 were selected to label DNA and the pentablock copolymer respectively in this study, because their non-overlapping spectra minimized the potential interference that could occur between the two dyes. Confocal images were collected with a Prairie Technologies Confocal Microscope (Prairie Technologies, Madison, WI) and analyzed with MetaView software (Universal Imaging Corporation). An argon/krypton mixed gas laser with 488 and 633 nm excitation lines was used to induce fluorescence. Excitation of EMA bound to DNA was achieved by using the 488 nm laser, with the emitted fluorescent wavelengths observed using a 600/40 nm notch filter. Alexa Fluor 647 attached to pentablock copolymer was excited by the 633 nm laser with the emitted fluorescent wavelengths observed using a 700/75 nm notch filter. The thickness of the cells was estimated by varying the scanning plane from the bottom to the top of the cells and images were collected at the central plane with optical sections of 0.5–0.7 μm.

Proliferation Measurement

Proliferation rate was expressed as the ratio of the number of daughter cells to the number of total cells and measured by counting cells stained with Brdu and DAPI. Brdu labeling was performed immediately following transfection by replacing the medium containing polyplexes with fresh growth medium containing 5 μM Brdu. After 18 h incubation, cells were fixed with 4% paraformaldehyde and stored in 1% paraformaldehyde at 4°C until performing immunocytochemistry.

Statistical Analysis

The data is presented as mean and standard deviation, which are calculated over at least three independent experiments. Significant differences between two groups were evaluated by Students' t test with $p \leq 0.05$ or $p < 0.1$, as specified.

RESULTS AND DISCUSSION

Transfection and Cytotoxicity Among Different Cell Types

In order to use the pentablock copolymers for cancer therapy, we tested the ability of the pentablock copolymer vectors to selectively transfect cancer cells (SKOV3) *versus* ARPE-19 cells using reporter genes (Fig. 1). Relative to the blank cells and naked DNA, polyplexes of P and P–F under different N/P ratio conditions exhibited up to three orders of magnitude higher efficiency in SKOV3 cells contrasting with the slight difference in ARPE-19 cells. ExGen, a linear polyethyleneimine vector, was used as a positive control, and did not exhibit a significant difference in transfection efficiency between the two different cell types, and the transfection efficiencies in both cell types were over three orders of magnitude higher than those of the negative controls. This demonstrates a potential selective transfection ability of the pentablock copolymer vectors compared to established vectors such as ExGen.

Although it is a commonly known fact that transfection efficiency could be largely dependent on cells due to the complex cellular structure and consequently varied gene delivery mechanisms, the big differences in transfection efficiencies of SKOV3 and ARPE-19 cells, which we may refer to as a cancer cell line and "normal" cell line respectively, provides a challenging possibility that this pentablock copolymer might possess a natural selectivity to transfect cancer cells or in general, the type of cells bearing some specific features of SKOV3 cells. Therefore, 3T3 cells were used to further test the transfection of normal cell lines mediated by pentablock copolymers. As shown in Fig. 2, similar to the case of APRE-19 cells, the pentablock copolymers lead to very low transfection efficiencies, almost comparable to those of blank cells, and ExGen still appeared to be a highly effective vector independent of the cell-line type. Therefore, the hypothesis that pentablock copolymers might specifically transfect the cancer cells sharing some key feature with SKOV3 cells was investigated further to determine if differences in proliferation rates of the different cell types were responsible for the differences in transfection efficiencies using the pentablock copolymers.

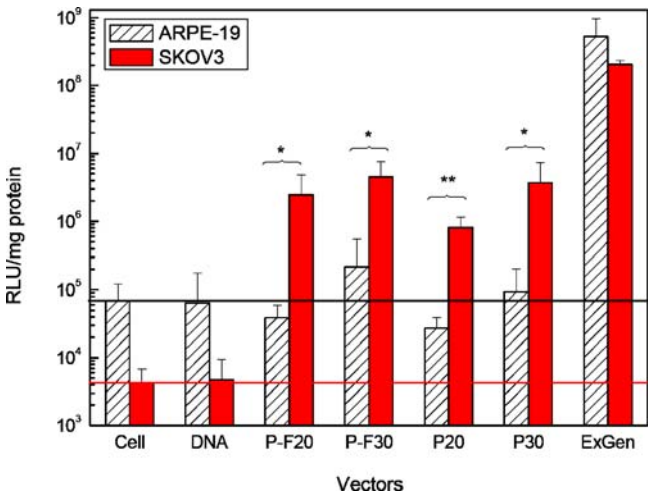

Fig. 1. Transfection of ARPE-19 and SKOV3 cells by P/DNA and P–F/DNA at N/P ratios of 20 and 30 as denoted by the figures following abbreviations. Blank cells and naked DNA were used as negative controls and ExGen at N/P ratio of 6 was used as the positive control according to the provided protocol. Luciferase activity was expressed as the relative light units (RLU) per milligram of protein (n=4, mean±SD. *$p \leq 0.05$, **$p < 0.01$).

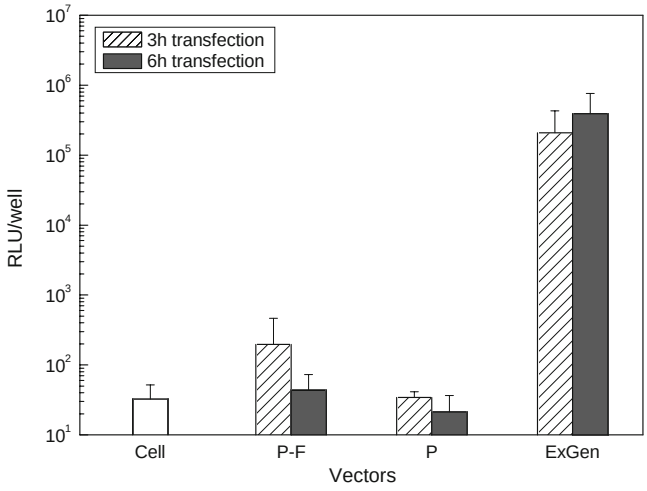

Fig. 2. Transfection of 3T3 cells by P/DNA and P–F/DNA at N/P ratios of 20 and by ExGen at N/P ratio of 6 for different transfection periods. Luciferase activity was expressed as relative light units (RLU) per well (n=4, mean±SD).

potentially change its physiochemical properties, the transfection efficiency and cytotoxicity of the dye labeled pentablock copolymer Pd was investigated. Fig. 3 indicates that there are indeed differences between Pd and the pentablock copolymer alone. Higher N/P ratios are required for Pd to obtain a similar level of gene expression as P does, which might be most likely due to the compromised DNA affinity by the dye attachment. There have been previous reports that oversubstitution of the molecular conjugates could interfere with the interaction of the polymers with DNA (33). In this case, the dye Alexa 647 attached to the end of polymer main chain could affect the polymer complexation with DNA in an unfavorable way, either by steric hindrance or by positive charge shielding. The Alexa 647 molecule (M_w=1250) accounts for ~50 wt.% of a PDEAEM block (M_w=2405 with 13 units), and together with the proximity between the dye and the tertiary nitrogen, it is reasonable to see a negative influence of Alexa 647 on transfection. However, it is interesting to point out that such a significant difference was brought about by only five percent of dye with respect to the pentablock copolymer. In addition to the DNA binding capability reduction by the conjugation of Alexa 647, the

Proliferation Measurement

The cell cycle mitotic phase has been reported to be a favorable period for nuclear transport using non-viral vectors (20). Although there are a number of intracellular barriers that work synergistically to cause a low level of gene expression relative to the DNA taken up by cells, usually less than 1% (30), the nuclear transport of polyplexes has been recognized as the rate-limiting step in DNA delivery (31), and has been found to be an important factor in the transfection of cell lines *versus* slow-dividing primary cells such as neurons. Hence, theoretically, the faster the cell proliferates, the greater the chances for DNA to enter into nuclei, and thereby the higher the gene expression would be. It was reported that gene expression was enhanced by enhancing cell proliferation with growth factor (32). To test the proliferation rates of the different cell types, Brdu was employed to stain the newly created cells with all nuclei labeled with DAPI. With the concern of minimizing the influence of host species on transfection characteristics, SKOV3 and ARPE-19 cells, which are both of human origin, were used for this study as opposed to the 3T3 cells which are mouse-derived. The test was conducted on transfected cells, in case the polyplexes have an effect on the proliferation. (Representative images shown in the Supplementary Figure 1). The proliferation rate was expressed as the number of daughter cells (pink) divided by the number of total cells (blue). The SKOV3 cells were found to proliferate significantly faster ($p<0.1$) than the ARPE-19 cells, with the rate of 54±15% *vs.* 25±12%. This potentially supports our hypothesis that the slower dividing rate of ARPE-19 cells probably resulted in less DNA importation to the nuclei of ARPE-19 cells and consequently to lower levels of gene expression.

To investigate this further, intercellular trafficking studies of pentablock copolymer/DNA polyplexes in SKOV3 and ARPE-19 cells were performed during transfection and post-transfection, by labeling the pentablock copolymer with a fluorescent dye. Since any modification to the polymer can

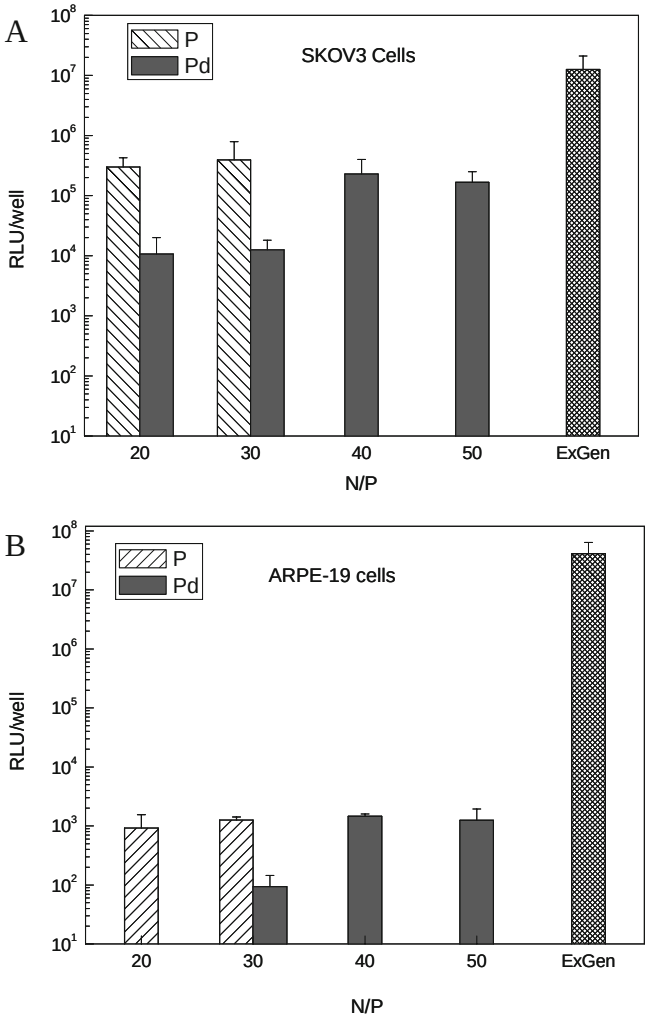

Fig. 3. Transfection of SKOV3 cells (**A**) and ARPE-19 cells (**B**) with the vector of P and Pd at various N/P ratios. (n=4, mean±SD).

resulting reduced charge density might also contribute to a lower cytotoxicity at a given N/P ratio.

Cytotoxicity Analysis Using LDH Assay

Cationic vectors can be cytotoxic, though the cytotoxicity of the pentablock copolymers can be tailored by adjusting the ratio of the cationic and non-cationic blocks in the copolymer (25). To evaluate the cell viability during the total transfection, an LDH assay was used. As shown in Fig. 4, the cytotoxicity of all the polyplexes is fairly acceptable for both SKOV3 and APRE-19 cells, expect for the P30 vector with the very high N/P ratio, and these two cell types seem to have a similar susceptibility to the vector. The vector of P–F with the Pluronic shielding the excess positive charges showed less damage to cells than the pentablock copolymer alone, suggesting that the shielding effect from F improved the biocompatibility of pentablock/DNA polyplexes. Cytotoxicity of Pd/DNA was indeed much lower than that of P/DNA counterparts for both cell types, which further proved the great influence of dye conjugation on the charge density. It was also found that interestingly, for both cell types, ExGen led to an even higher toxicity in the later 45 h of post-transfection relative to the first 3 h, while most of pentablock copolymer polyplexes seemed to act differently. It is worth noting that for the polyplexes such as P30/DNA that exhibited a high toxicity in the first 3 h transfection, there was not much additional cytotoxicity in the next 45 h.

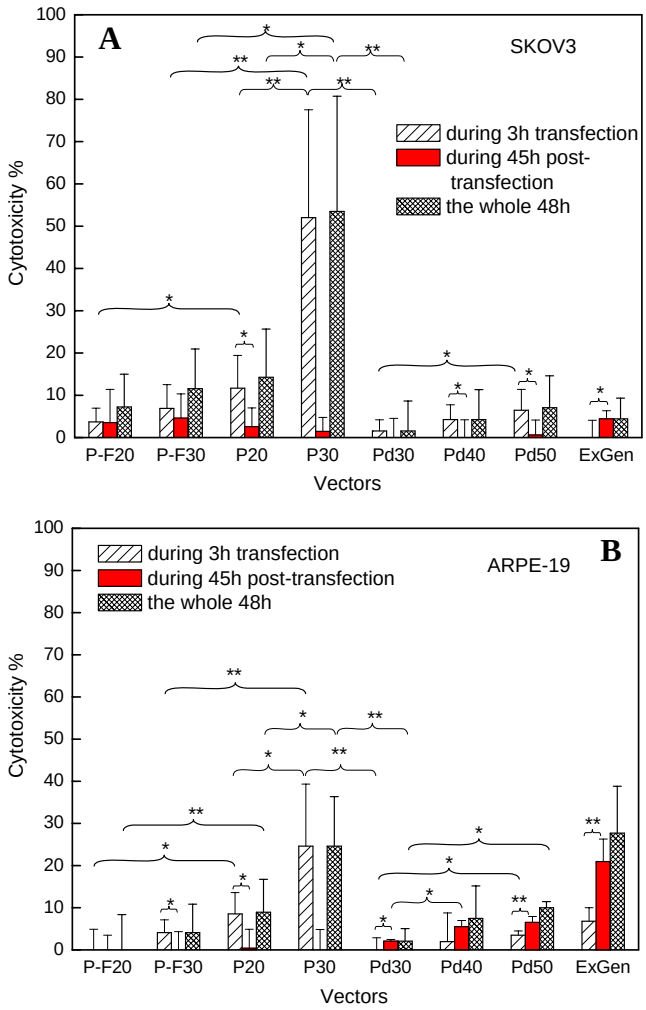

Fig. 4. Cytotoxicity of polyplexes on SKOV3 (**A**) and ARPE-19 cells (**B**) with LDH assay at various N/P ratio as denoted by the figures following abbreviations. ($n=4$, mean±SD. $*p \le 0.05$, $**p < 0.01$). ExGen was used at N/P ratio of 6 according to the provided protocol.

ExGen carries plenty of primary and secondary amines and is known to be much more cytotoxic than complexed ExGen where most charges of amines have been neutralized by DNA; moreover, the membrane destabilization effect (34) of free PEI and its interference with transcriptional and translational processes (35) might also account for its toxicity. On the other hand, the intense charge density of PEI would not allow the release of the DNA cargo readily, so the ExGen/DNA polyplexes showed a slower toxicity rather than a quick one, which is in good agreement with the report by Godbey and co-workers (35). However, transgene vectors with tertiary amines as the functional moieties like pentablock copolymers, have been reported to be less toxic than those with primary residues like PEI (26,36). Therefore, even after uncomplexing from DNA they did not show as much long-term toxicity as ExGen, instead showing an initial cytotoxicity during the first 3 h probably due to relatively larger percentage of uncomplexed polymer at a given higher N/P ratio or the relatively faster release of DNA. However, the cytotoxicity of Pd/DNA was found to show a different trend during the whole transfection process compared to P/DNA in the ARPE-19 cells, with higher cytotoxicity in the post-transfection stage than that in the transfection period. If the uncomplexed Pd is presumed to be a major source of cytotoxicity, apart from the membrane damage during cellular entry, there should be more uncomplexed Pd in the later 45 h post-transfection in ARPE-19 cells relative to SKOV3 cells where nearly no cytotoxicity was observed. This implies that some intracellular differences between the two cell types may affect the relatively weak complexation of Pd and DNA, which was investigated in the intracellular trafficking studies of the polyplexes. Taking the transfection efficacy and cytotoxicity into account, Pd at an N/P ratio of 40 was used for the intracellular trafficking study.

Intracellular Trafficking of Pd/DNA Polyplexes

Based on the proliferation results that showed that SKOV3 cells proliferate faster than ARPE-19 cells, our initial hypothesis was that the significant differences in transfection efficacy between the two cell lines were largely due to the positive effect of proliferation rate on nuclear transport. To check if nuclear uptake actually occurs more in SKOV3 cells than in ARPE-19 cells, pentablock copolymer/DNA polyplexes were tracked at 3, 10 and 24 h after the start of transfection. Fig. 5 shows a representative image of the APRE-19 cells at 3 h, where colocalization of pentablock copolymer and DNA was clearly observed with yellow dots, suggesting that polyplexes remained in their original form, and in particular some polyplexes had localized to the perinucleus as seen in cells 1, 3, and 4. However, the most impressive feature of the 3 h sample resides in the dissociated polyplexes which could be easily detected by the abundant red, and relatively fewer green dots. Moreover, except for cells 3 and 4, the red free pentablock copolymer appeared to

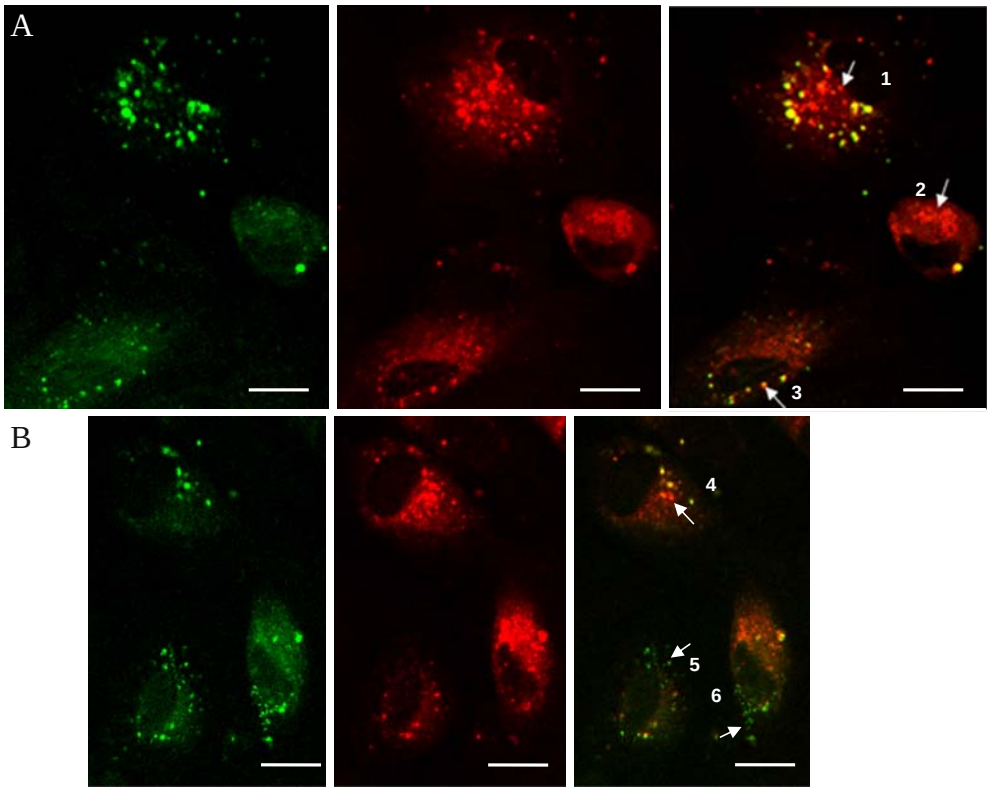

Fig. 5. Confocal images from labeled pentablock copolymers and DNA in ARPE-19 cells 3 h after transfection. *Images on the left colored green* represent DNA, the *center ones colored red* represent the pentablock copolymers and the *images on the right* are the alignment of the other two images. Panel **A** and panel **B** are from different observation spots. Scale bar is 20 μm.

be dominant and the green DNA was just absent, especially in cells 1 and 2. We have postulated two possible reasons for the absence of the free DNA. One possibility is that DNA was degraded by the nuclease in the cytosol, and the other is that the DNA was exported out of the cell. The appearance of strong red and weak green signals has been found to be typical among all the images), which may imply that the DNA is subjected to degradation during or after release from the polyplexes. This was proved by testing the intensity of fluorescence of DNA-EMA and degraded DNA-EMA (shown in Supplementary Figure 2), and by integrating within the range of the filter from 580 to 620 nm. It was found that the untreated DNA-EMA was as twice fluorescent as the degraded one. It was once reported that the digestion of EMA labeled RNA induced a 14-fold decrease in the fluorescence intensity (37). Therefore, the free DNA was not totally absent as it appeared to be in the aligned images, but had probably been degraded by the nucleases to some extent and showed less intense fluorescence compared to the bright red fluorescence from pentablock copolymer.

When focusing on cells 5 and 6, free DNA was found localized around the cell membrane or close to the mem-

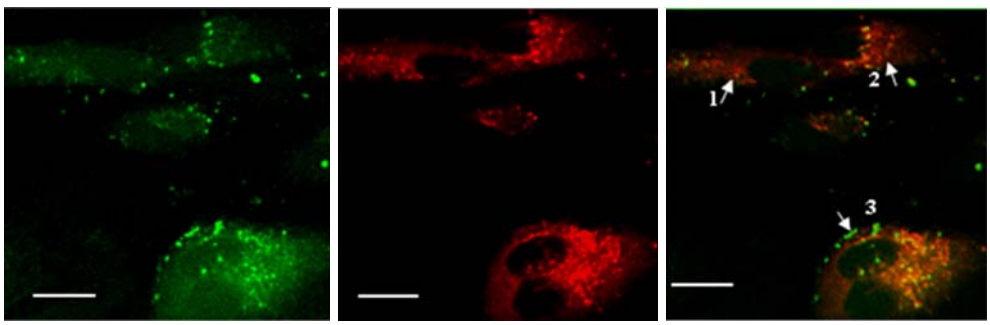

Fig. 6. Confocal images from labeled pentablock copolymer and DNA in ARPE-19 cells 10 h after transfection. *Image on the left colored green* represents DNA, the *center one colored red* represents the pentablock copolymers and the *image on the right* is the alignment of the other two images. Scale bar is 20 μm.

brane, potentially awaiting transportation out of the cell. This feature was also found commonly in the 10 h samples as it was shown in the representative cell 3 of Fig. 6, where free DNA accumulated along the outer membrane or may be sequestrated by the cell membrane. The nearly doubled nucleus and the incompletely separated nuclear envelope of cell 3, as indicated by the lower arrow, demonstrates an obvious late mitosis phase—telophase. Moreover, DNA and pentablock polymer have been observed in the dividing nucleus with non-perfect colocalization, suggesting that they both either entered into the nucleus in an uncomplexed form or dissociated from each other after nuclear entry as polyplexes. But the large number of polyplexes accumulating right outside the nucleus, as well as the small amount of free DNA observed, point to the second possibility. The intranuclear DNA and pentablock copolymer are close to the dividing area, indicating that the nuclear entry possibly took place during the nuclear division and may have been facilitated by nuclear membrane breakdown (21). In addition, the feature of strong red and weak green was also found in this 10 h sample as shown by arrows in cells 1 and 2. Therefore, by comparing the cells after 3 h transfection, and those after another 7 h posttransfection, the latter showed an enhanced nuclear uptake probably due to the mitotic activity, but maintained the appearance of dominant red fluorescence. This implies that the DNA might be degraded after uncomplexation, and the accumulation of DNA close to or even at the cell membrane suggests a possible export mechanism from the cell. When post-transfection time was extended to 21 h as seen in Fig. 7, the transfected cells exhibited an increased amount of DNA in the nuclei either complexed or uncomplexed as shown in cells 3, 4 and 5. The other features were consistent with the previous two time points concerning varied intensity of green fluorescence from DNA and membrane concentrated distribution of DNA, as especially indicated with the arrow in cell 2.

The polyplexes, however, had a totally different intracellular route in SKOV3 cells as shown in Fig. 8. A large quantity of fairly good colocalization of green and red dots especially in panel A suggests that DNA was still effectively protected from degradation in the well maintained polyplexes. More importantly, polyplexes had localized into nuclei in considerable numbers at 3 h after transfection which is dramatically higher than the cases of all APRE-19 cell samples in test, and which might be contribute to the differences in the transfection efficacy of the pentablock copolymers between the two cell types. Besides, all of the DNA and pentablock copolymers have been shown to be perfectly overlaid in panel A; therefore the polyplexes in the nuclei are the ones originally present in the cytoplasm rather than being reformed by the DNA and pentablock copolymers that entered into the nuclei separately. Therefore, at least a portion of DNA is transported into nuclei complexed with the pentablock copolymer. There is a possibility of uncom-

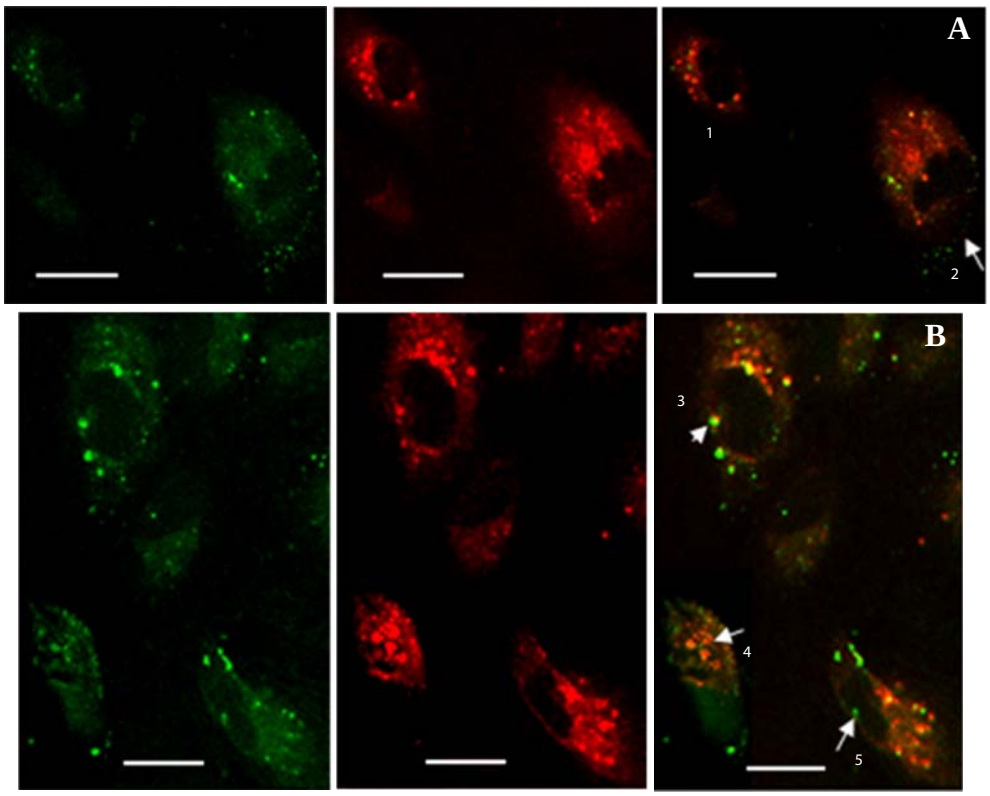

Fig. 7. Confocal images from labeled pentablock copolymer and DNA in ARPE-19 cells 24 h after transfection. *Images on the left colored green* represent DNA, the *center ones colored red* represent the pentablock copolymers and the *images on the right* are the alignment of the other two images. Panel **A** and panel **B** are from different observation spots. Scale bar is 20 μm.

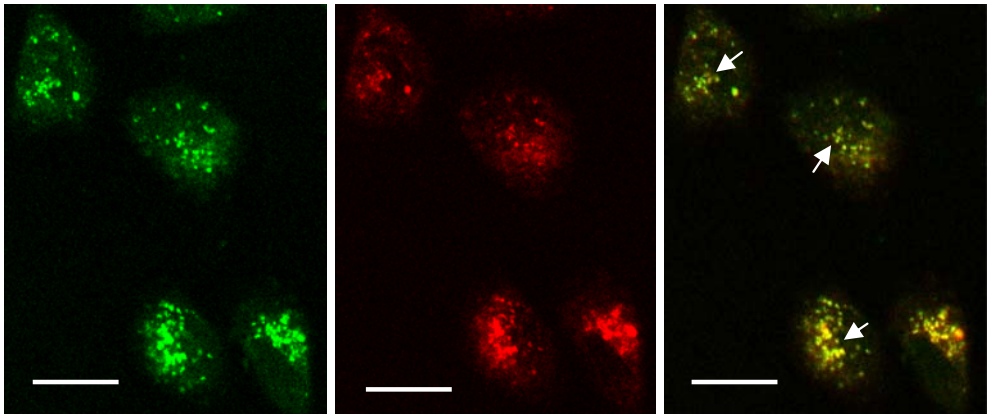

Fig. 8. Confocal images from labeled pentablock copolymer and DNA in SKOV3 cells 3 h after transfection. *Images on the left colored green* represent DNA, the *center ones colored red* represent the pentablock copolymers and the *images on the right* are the alignment of other two images. Scale bar is 20 μm.

plexed DNA entering the nucleus as well, since plasmid DNA has been well known to be able to enter into the nuclei (30). But considering the degradation by nucleases (38) and the low diffusion rate caused by the hindrance of cytoskeleton and binding with other cytoplasmic elements (39), the free DNA would have a small chance to successfully locate into the nuclei.

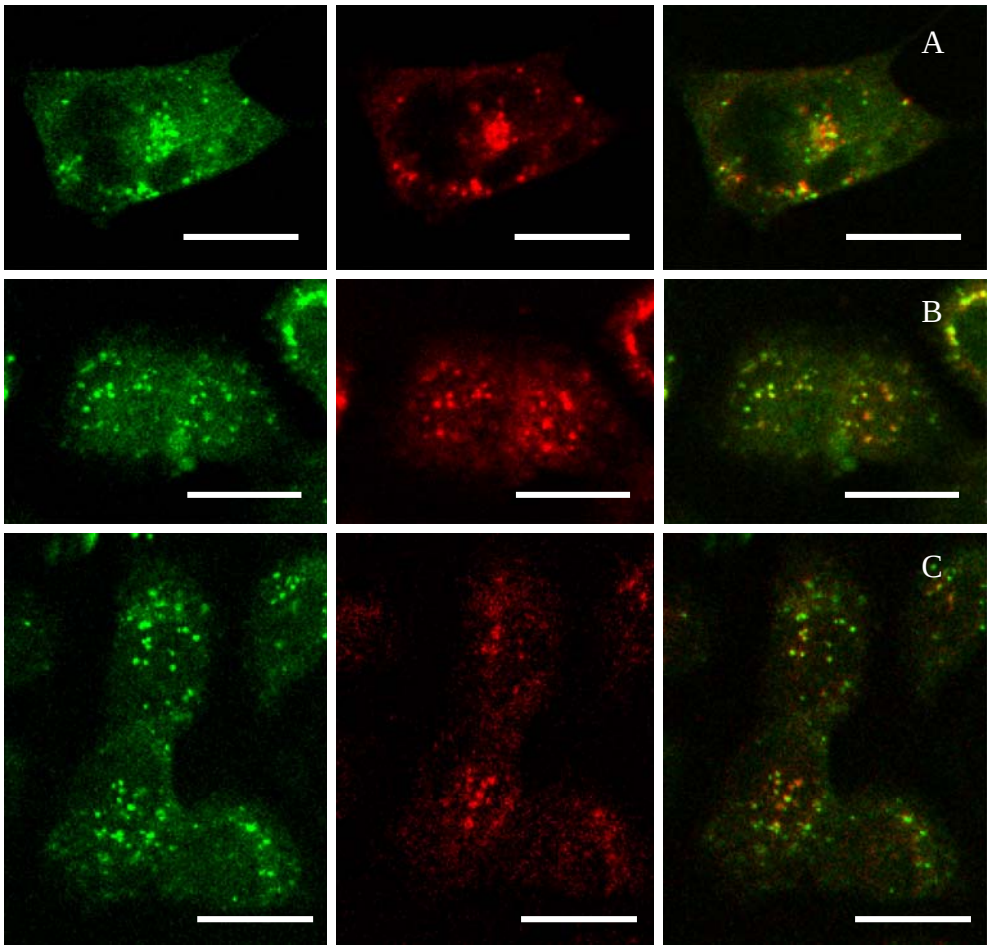

Fig. 9. Nuclear transport of polyplexes during mitosis from SKOV3 cells after 3 h transfection. *Images on the left colored green* represent DNA, the *center ones colored red* represent the pentablock copolymers and the *images on the right* are the alignment of other two images. Panels **A**, **B** and **C** are from different observation spots. Scale bar is 20 μm.

As SKOV3 cells proliferate faster than the ARPE-19 cells, the higher transfection efficiency of SKOV3 cell line was hypothesized to result from its consequently facilitated nuclear uptake. The nuclear uptake of polyplexes appeared to be common in SKOV3 cells samples, even as early as 3 h after transfection. Panels A to C in Fig. 9 might represent three different stages in mitosis according to the varied appearance of nuclei. Although it is hard to say at which exact stage each set of cells is in, they all seem to be after prometaphase, during which the disintegration of the nuclear membrane occurs. That is probably the reason why each nucleus undergoing division shows polyplexes inside. Since similar phenomena were just observed less frequently in the ARPE-19 cells 10 h after transfection, the slower dividing rate could largely account for the lower transfection efficiency.

The SKOV3 samples for 10 h and 24 after transfection look similar to those of 3 h (Fig. 10), except for the less perfect colocalization and more free DNA in the nuclei, which is reasonable as the dissociation can be expected to develop over time. However, relative to the rare colocalization at the same time points in ARPE-19 cells, the tight binding in SKOV3 cells implied a long-term protection provided by the pentablock copolymer. This agrees well with LDH results regarding the cytotoxicity of Pd/DNA in post-transfection, which appears to be proportional to the amount of uncomplexed Pd. Although long-term protection might reduce the cytotoxicity as well as the loss of DNA, the relatively few DNA released for further transcription and translation might present a potential bottleneck to gain higher gene expression. Therefore, the differences in transfection

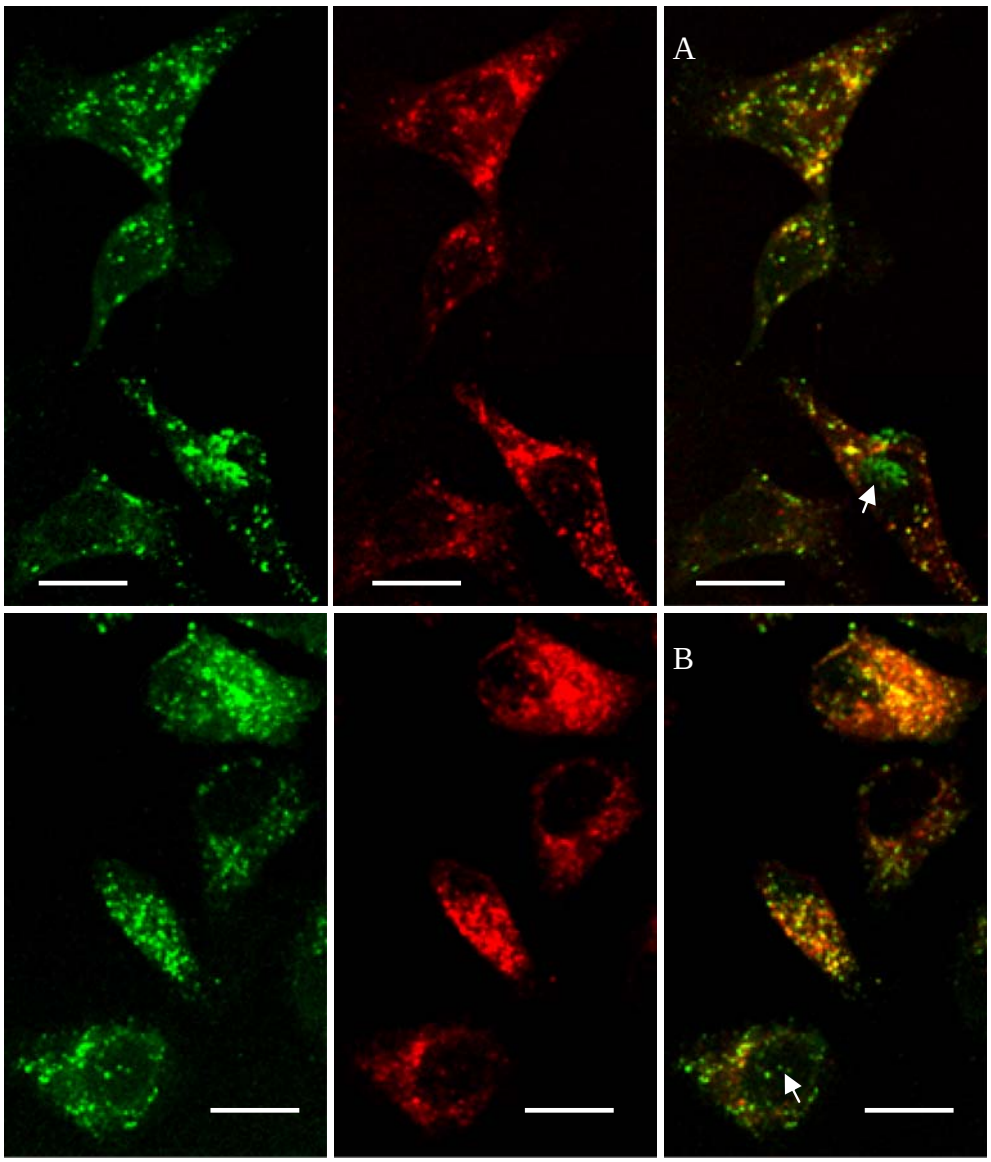

Fig. 10. Confocal images from labeled pentablock copolymer and DNA in SKOV3 cells 10 h (panel **A**) and 24 h (panel **B**) after transfection. *Images on the left colored green* represent DNA, *center ones colored red* represent the pentablock copolymers and the *images on the right* are the alignment of the other two images. Panel **A** and panel **B** are from different observation spots. Scale bar is 20 μm.

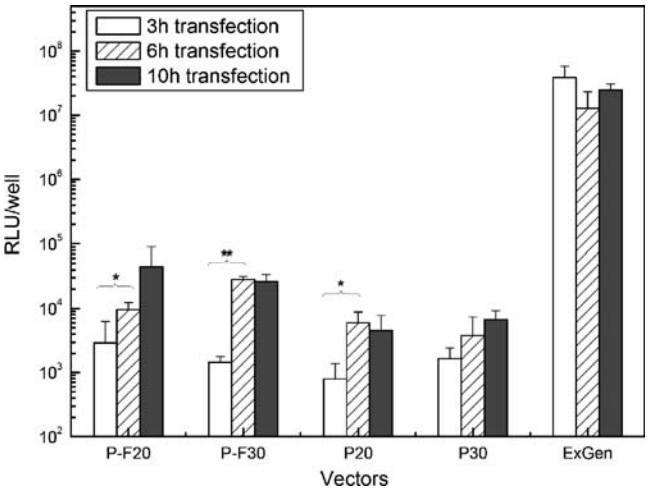

Fig. 11. Transfection of ARPE-19 cell line by P/DNA and P–F/DNA polyplexes with different transfection period at N/P ratio of 20 and 30 as denoted by the figures following abbreviations. ExGen was used as a positive control at N/P ratio of 6 according to the provided protocol. Luciferase activity was expressed as the relative light unit (RLU) per well (n=4, mean±SD. *$p \leq 0.05$, **$p < 0.01$).

efficiency between ARPE-19 and SKOV3 cell lines might be due to the lower proliferation rate of the ARPE-19 cells, thereby lowering nuclear uptake. Although the exogenous material can definitely achieve the nuclear import in the interphase cells through the nuclear membrane embedded nuclear pore complex (NPC) (40), the hourglass-like NPC cannot allow large cargo to transit though passively (41)with the midplane as narrow as 40 nm (42). The inclusion of nuclear localization signal (NLS) in the vector could facilitate the transit and to some extent enhance the size limit up to 60 nm, but the polyplexes sized around 150 nm are still excluded (43). Thus even with a NLS, the polyplexes are still too large to be imported into the nucleus (31). Since our pentablock copolymer/DNA polyplexes formed at N/P ratios of 20 have a size distribution ranging from 100 to 500 nm in serum supplemented growth media (data not shown), and do not possess any NLS moieties, it would be difficult for them to traverse the nuclear membrane through NPC even though opportunities exist to bind with the intracellular NLS. In this case, the more realistic strategy of nuclear localization should be the entry after nuclear breakdown in mitosis. The more often cells experience a mitotic phase, the more DNA could be transported into the nuclei to get more genes expressed. Based on the fact that much more DNA either complexed or uncomplexed has been found in the nuclei of faster dividing SKOV3 cells, the higher level of gene expression in SKOV3 with respect to ARPE-19 cell line is related to the faster proliferation rate of the SKOV3 cells.

To test this assumption further, we extended the duration of transfection of ARPE-19 cells to 6 h (Fig. 11) and found that the gene expression mediated by most of the pentablock copolymer vectors was enhanced to a significantly higher level relative to the case of 3 h transfection, suggesting more DNA has been available for the cells in mitosis. The exception of P30 and ExGen might be due to the negative effect of the accompanying increased cytotoxicity especially at higher N/P ratios. In addition to this cause, the excellent nuclear delivery ability of ExGen could make it benefit little from lengthened transfection. Further extending transfection to 10 h, resulted in no significant differences. Apart from causing increased cytotoxicity, cells might have been too confluent to proliferate any further to aid in nuclear uptake. Secondarily the intracellular DNA in ARPE-19 cells was found to be much lesser than that in SKOV3 cells, which may be directly caused by the less effective cellular uptake, or probably due to the degradation of DNA by the nuclease in lysosome or cytoplasm, or due to the exocytosis of DNA. Consequently, the limited amount of DNA available in cytoplasm further inhibited the nuclear transport. In the SKOV3 images, the polyplexes were dominant in the cytoplasm

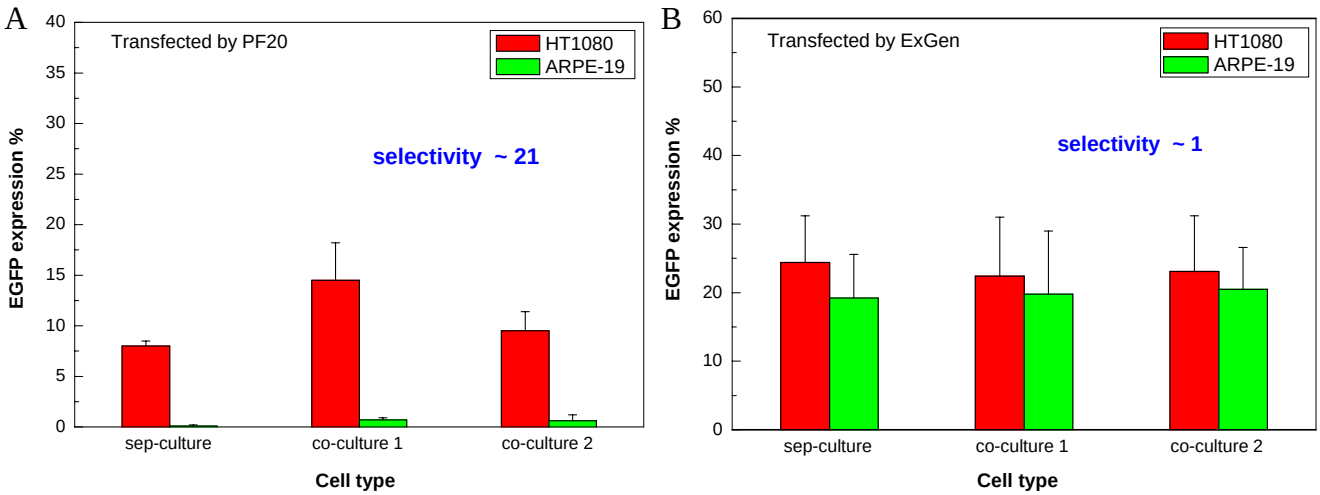

Fig. 12. EGFP expression in co-cultured HT1080/ARPE-19 cells mediated by PF at N/P ratio of 20 (**A**) and ExGen at N/P ratio of 6 (**B**). Selectivity was expressed as the ratio of percentage of cells with EGFP expression in cancerous HT1080 cells over the percentage in ARPE-19 cells. Co-culture 1 and co-culture 2 indicate two co-culture conditions in which HT1080 and ARPE-19 cells were initially seeded at ratios of 1:2 and 1:3, respectively. Sep-culture represents the transfection performed on individually cultured cells as opposed to co-cultures.

especially at 3 h indicating that almost all the intracellular pentablock copolymers were complexed with DNA when entering into cells. Since the amount of pentablock copolymer in SKOV3 and ARPE-19 cells have not been found to be very different, the less powerful cellular uptake may just partially explain the small quantity of DNA in ARPE-19 cells. The degradation and exocytosis of DNA are also possibilities. After being internalized via endocytosis which is known as the major, if not the sole mode of cellular entry (20), the polyplexes are trapped in the early endosomes. These early endosomes either fuse with each other to form late endosomes and subsequently endo-lysosomes by fusing with lysosomes or recycle their contents back to the cell surface (44). The endocytosed polyplexes are accordingly subjected to three fates, being recycled to plasma membrane and subsequent exocytosis, released into cytoplasm, or delivered to endo-lysosomes via late endosomes (39). Although the degradation most likely takes place in endolysosomes (45), the escape might also be facilitated by the lower pH (~5.0) of endolysosomes (46). Polyplexes released into cytoplasm still encounter diffusional barriers to traverse the highly crowded cytoplasm (47), and metabolic barriers to maintain DNA intact before eventually localizing into the nucleus. It has also been reported that the intracellular barriers to DNA transfer vary with cell type (20,22). Therefore, under the intracellular environment of APRE-19 cells, the binding affinity of the internalized polyplexes might be reduced, which in turn caused more DNA to be degraded or released. The released DNA again could be degraded during the long journey to the nucleus. As a result, lesser DNA was observed in ARPE-19 cells than in SKOV3 cells.

Transfection of Co-cultured HT1080/ARPE-19 Cells

The selectivity that potentially between cancer and normal cells transfected with pentablock copolymer polyplexes was further studied on another carcinoma cell line HT1080 by co-culturing it with ARPE-19. In this manner both qualitative and quantitative data can be obtained in an environment closer to the *in vivo* situation. Consistent with the earlier results obtained using separate cultures of different cell lines, the pentablock copolymers showed selectivity of transfection of cancer cells even in co-culture with non-cancerous cells. EGFP expression was seen only in the HT1080 cells even though they were fewer in number relative to the ARPE-19 cells (see Supplementary Figure 3). For the transfection mediated by ExGen, however, EGFP was evenly expressed in both of these two cell types (see Supplementary Figure 4), indicating that the transfection efficacy of ExGen is indeed independent of cell type. This finding was further confirmed and quantified with flow cytometry (Fig. 12) where the selectivity of transfection of cancer cells using the pentablock copolymer vectors was around 21 whereas no selectivity was exhibited in the transfection mediated by ExGen. Since HT1080 cells were found to proliferate even faster than SKOV3 cells (data not shown here), this selectivity obtained using the pentablock copolymer mediated transfection could be related to the proliferation rate.

CONCLUSIONS

In summary, we have reported an interesting finding that the pentablock copolymer-mediated transfection was significantly higher in the cancerous SKOV3 and HT1080 cell lines as compared to the non-cancerous APRE-19 and 3T3 cell lines, which implies that they may possess natural transfection selectivity for specific cell types. Through proliferation measurements and confocal microscopy-based trafficking studies, the faster proliferation rate of SKOV3 cells and the more formidable intracellular barriers of APRE-19 cells were found to contribute to this result. The selectivity was found to be about 21 for the transfection efficiency of HT1080 cells over that of APRE-19 cells using pentablock copolymers. However, the well-known and commonly used transgene vector ExGen induced an almost evenly high transfection in all cell types in this study and did not show any selectivity. Since primary cells typically have even slower proliferation rates than most cell lines, the pentablock copolymers are expected to have a better selectivity between carcinoma and primary normal cells, thereby providing an excellent vector to deliver genes for cancer therapies.

ACKNOWLEDGMENTS

We would like to acknowledge financial support from the Bailey Career Development grant and a NSF-REU grant. We would also like to thank Marit Nilsen-Hamilton for providing 3T3 cells. Mallapragada would like to dedicate this manuscript to Prof. Nicholas Peppas for his exceptional guidance, mentoring and friendship.

REFERENCES

1. J. C. Perales, T. Ferkol, M. Molas, and R.W. Hanson. An evaluation of receptor-mediated gene transfer using synthetic DNA-ligand complexes. *Eur. J. Biochem.* **226**:255–266 (1994). Medline. doi:10.1111/j.1432-1033.1994.tb20049.x.
2. H. Lee, T. H. Kim, and T. G. Park. A receptor-mediated gene delivery system using streptavidin and biotin-derivatized, pegylated epidermal growth factor. *J. Control. Release.* **83**:109–119 (2002). Medline. doi:10.1016/S0168-3659(02)00166-9.
3. L. Jabr-Milane, L. van Vlerken, H. Devalapally, D. Shenoy, S. Komareddy, M. Bhavsar, and M. Amiji. Multi-functional nanocarriers for targeted delivery of drugs and genes. *J. Control. Release.* 130:121–128 (2008).
4. K. Koike, T. Hara, Y. Aramaki, S. Takada, and S. Tsuchiya. Receptor-mediated gene transfer into hepatic cells using asialoglycoprotein-labeled liposomes. *Ann. N. Y. Acad. Sci.* **716**:331–333 (1994). Medline. doi:10.1111/j.1749-6632.1994.tb21725.x.
5. C. Plank, K. Zatloukal, M. Cotten, K. Mechtler, and E. Wagner. Gene transfer into hepatocytes using asialoglycoprotein receptor mediated endocytosis of DNA complexed with an artificial tetraantennary galactose ligand. *Bioconjugate. Chem.* **3**:533–539 (1992). Medline. doi:10.1021/bc00018a012.
6. K. Chul Cho, J. Hoon Jeong, H. Jung Chung, C. O Joe, S. Wan Kim, and T. Gwan Park. Folate receptor-mediated intracellular delivery of recombinant caspase-3 for inducing apoptosis. *J. Control. Release.* **108**:121–131 (2005). Medline. doi:10.1016/j.jconrel.2005.07.015.
7. W. Wijagkanalan, S. Kawakami, M. Takenaga, R. Igarashi, F. Yamashita, and M. Hashida. Efficient targeting to alveolar macrophages by intratracheal administration of mannosylated liposomes in rats. *J. Control. Release.* **125**:121–130 (2008). Medline. doi:10.1016/j.jconrel.2007.10.011.

8. I. Y. Park, I. Y. Kim, M. K. Yoo, Y. J. Choi, M. -H. Cho, and C. S. Cho. Mannosylated polyethylenimine coupled mesoporous silica nanoparticles for receptor-mediated gene delivery. *Int. J. Pharm.* **359**:280–287 (2008). Medline. doi:10.1016/j.ijpharm.2008.04.010.
9. J. H. Wong, H. Y. E. Chan, and T. B. Ng. A mannose/glucose-specific lectin from Chinese evergreen chinkapin (*Castanopsis chinensis*). *Biochim. Biophys. Acta* (*BBA*)-*General Subjects*. **1780**:1017–1022 (2008).
10. Y. Li, M. Ogris, E. Wagner, J. Pelisek, and M. Rüffer. Nanoparticles bearing polyethyleneglycol-coupled transferrin as gene carriers: preparation and *in vitro* evaluation. *Int. J. Pharm.* **259**:93–101 (2003). Medline. doi:10.1016/S0378-5173(03)00211-4.
11. C. R. Dass, and P. F. M. Choong. Selective gene delivery for cancer therapy using cationic liposomes: *in vivo* proof of applicability. *J. Control. Release*. **113**:155–163 (2006). Medline. doi:10.1016/j.jconrel.2006.04.009.
12. X. B. Zhao, and R. J. Lee. Tumor-selective targeted delivery of genes and antisense oligodeoxyribonucleotides via the folate receptor. *Adv. Drug Deliv. Rev.* **56**:1193–1204 (2004). Medline. doi:10.1016/j.addr.2004.01.005.
13. B. Liang, M. -L. He, Z. -P. Xiao, Y. Li, C. -Y. Chan, H. -F. Kung, X. -T. Shuai, and Y. Peng. Synthesis and characterization of folate-PEG-grafted-hyperbranched-PEI for tumor-targeted gene delivery. *Biochem. Biophys. Res. Commun.* **367**:874–880 (2008). Medline. doi:10.1016/j.bbrc.2008.01.024.
14. S. Kawakami, S. Fumoto, M. Nishikawa, F. Yamashita, and M. Hashida. *In vivo* gene delivery to the liver using novel galactosylated cationic liposomes. *Pharm. Res.* **17**:306–313 (2000). Medline. doi:10.1023/A:1007501122611.
15. S. Fumoto, F. Nakadori, S. Kawakami, M. Nishikawa, F. Yamashita, and M. Hashida. Analysis of hepatic disposition of galactosylated cationic liposome/plasmid DNA complexes in perfused rat liver. *Pharm. Res.* **20**:1452–1459 (2003). Medline. doi:10.1023/A:1025766429175.
16. K. Corsi, F. Chellat, L. Yahia, and J. C. Fernandes. Mesenchymal stem cells, MG63 and HEK293 transfection using chitosan–DNA nanoparticles. *Biomaterials*. **24**:1255–1264 (2003). Medline. doi:10.1016/S0142-9612(02)00507-0.
17. S. -W. Kim, T. Ogawa, Y. Tabata, and I. Nishimura. Efficacy and cytotoxicity of cationic-agent-mediated nonviral gene transfer into osteoblasts. *J. Biomed. Mater. Res. Part A*. **71A**:308–315 (2004). doi:10.1002/jbm.a.30160.
18. H. Shen, J. Tan, and W. M. Saltzman. Surface-mediated gene transfer from nanocomposites of controlled texture. *Nat Mater.* **3**:569–574 (2004). Medline. doi:10.1038/nmat1179.
19. I. Mortimer, P. Tam, I. MacLachlan, R. W. Graham, E. G. Saravolac, and P. B. Joshi. Cationic lipid-mediated transfection of cells in culture requires mitotic activity. *Gene Therapy.* **6**:403–411 (1999). Medline. doi:10.1038/sj.gt.3300837.
20. A. Remy-Kristensen, J. -P. Clamme, C. Vuilleumier, J. -G. Kuhry, and Y. Mely. Role of endocytosis in the transfection of L929 fibroblasts by polyethylenimine/DNA complexes. *Biochim. Biophys. Acta, Biomembr.* **1514**:21–32 (2001). doi:10.1016/S0005-2736(01)00359-5.
21. S. Brunner, T. Sauer, S. Carotta, M. Cotten, M. Saltik, and E. Wagner. Cell cycle dependence of gene transfer by lipoplex, polyplex and recombinant adenovirus. *Gene Ther.* **7**:401–407 (2000). Medline. doi:10.1038/sj.gt.3301102.
22. H. Pollard, J. -S. Remy, G. Loussouarn, S. Demolombe, J. -P. Behr, and D. Escande. Polyethylenimine but not cationic lipids promotes transgene delivery to the nucleus in mammalian cells. *J. Biol. Chem.* **273**:7507–7511 (1998). Medline. doi:10.1074/jbc.273.13.7507.
23. M. D. Determan, J. P. Cox, S. Seifert, P. Thiyagarajan, and S. K. Mallapragada. Synthesis and characterization of temperature and pH-responsive pentablock copolymers. *Polymer.* **46**:6933–6946 (2005). doi:10.1016/j.polymer.2005.05.138.
24. A. V. Kabanov, E. V. Batrakova, and V. Y. Alakhov. Pluronic(R) block copolymers as novel polymer therapeutics for drug and gene delivery. *J. Control. Release*. **82**:189–212 (2002). Medline. doi:10.1016/S0168-3659(02)00009-3.
25. A. Agarwal, R. Unfer, and S. K. Mallapragada. Novel cationic pentablock copolymers as non-viral vectors for gene therapy. *J. Control. Release*. **103**:245–258 (2005). Medline. doi:10.1016/j.jconrel.2004.11.022.
26. A. Agarwal, R. C. Unfer, and S. K. Mallapragada. Investigation of *in vitro* compatibility of novel pentablock copolymers for gene delivery. *J. Biomed. Mater. Res*. **81A**:24–39 (2007). doi:10.1002/jbm.a.30920.
27. W. T. Godbey, K. K. Wu, and A. G. Mikos. Tracking the intracellular path of poly(ethylenimine)/DNA complexes for gene delivery. *Proc. Natl. Acad. Sci U. S. A*. **96**:5177–5181 (1999). Medline. doi:10.1073/pnas.96.9.5177.
28. T. Serikawa, N. Suzuki, H. Kikuchi, K. Tanaka, and T. Kitagawa. A new cationic liposome for efficient gene delivery with serum into cultured human cells: a quantitative analysis using two independent fluorescent probes. *Biochim.Biophys. Acta, Biomembr.* **1467**:419–430 (2000). doi:10.1016/S0005-2736(00)00239-X.
29. M. Ruponen, S. Ronkko, P. Honkakoski, J. Pelkonen, M. Tammi, and A. Urtti. Extracellular glycosaminoglycans modify cellular trafficking of lipoplexes and polyplexes. *J. Biol. Chem*. **276**:33875–33880 (2001). Medline. doi:10.1074/jbc.M011553200.
30. M. E. Dowty, P. Williams, G. Zhang, J. E. Hagstrom, and A. W. Jon. Plasmid DNA entry into postmitotic nuclei of primary rat myotubes. *Proc. Natl. Acad. Sci. U. S. A*. **92**:4572–4576 (1995). Medline. doi:10.1073/pnas.92.10.4572.
31. C. W. Pouton, K. M. Wagstaff, D. M. Roth, G. W. Moseley, and D. A. Jans. Targeted delivery to the nucleus. *Adv. Drug Deliv. Rev*. **59**:698–717 (2007). Medline. doi:10.1016/j.addr.2007.06.010.
32. K. W. Riddle, H. -J. Kong, J. K. Leach, C. Fischbach, C. Cheung, K. S. Anseth, and D. J. Mooney. Modifying the proliferative state of target cells to control DNA expression and identifying cell types transfected *in vivo*. *Mol. Ther.* **15**:361–368 (2007).
33. A. -G. Ziady, T. Ferkol, T. Gerken, D. V. Dawson, D. H. Perlmutter, and P. B. Davis. Ligand substitution of receptor targeted DNA complexes affects gene transfer into hepatoma cells. *Gene Ther.* **5**:1685–1697 (1998). Medline. doi:10.1038/sj.gt.3300777.
34. I. M. Helander, H. -L. Alakomi, K. Latva-Kala, and P. Koski. Polyethyleneimine is an effective permeabilizer of Gram-negative bacteria. *Microbiology.* **143**:3193–3199 (1997).
35. W. T. Godbey, K. K. Wu, and A. G. Mikos. Poly(ethylenimine)-mediated gene delivery affects endothelial cell function and viability. *Biomaterials*. **22**:471–480 (2001). Medline. doi:10.1016/S0142-9612(00)00203-9.
36. D. Fischer, Y. Li, B. Ahlemeyer, J. Krieglstein, and T. Kissel. *In vitro* cytotoxicity testing of polycations: influence of polymer structure on cell viability and hemolysis. *Biomaterials*. **24**:1121–1131 (2003). Medline. doi:10.1016/S0142-9612(02)00445-3.
37. P. H. Boltont, and D. R. Kearns. Spectroscopic properties of ethidium monoazide: a fluorescent photoaffmity label for nucleic acids. *Nucleic Acids Res*. **5**:4891–4903 (1978). Medline. doi:10.1093/nar/5.12.4891.
38. M. F. Bureau, S. Naimi, R. Torero Ibad, J. Seguin, C. Georger, E. Arnould, L. Maton, F. Blanche, P. Delaere, and D. Scherman. Intramuscular plasmid DNA electrotransfer: biodistribution and degradation. *Biochim. Biophys. Acta, Gene Struct. Expr.* **1676**:138–148 (2004).
39. D. Lechardeur, A. S. Verkman, and G. L. Lukacs. Intracellular routing of plasmid DNA during non-viral gene transfer. *Adv. Drug Deliv. Rev*. **57**:755–767 (2005). Medline. doi:10.1016/j.addr.2004.12.008.
40. G. Liu, D. Li, M. K. Pasumarthy, T. H. Kowalczyk, C. R. Gedeon, S. L. Hyatt, J. M. Payne, T. J. Miller, P. Brunovskis, T. L. Fink, O. Muhammad, R. C. Moen, R. W. Hanson, and M. J. Cooper. Nanoparticles of compacted DNA transfect postmitotic cells. *J. Biol. Chem*. **278**:32578–32586 (2003). Medline. doi:10.1074/jbc.M305776200.
41. N. Pante, and M. Kann. Nuclear pore complex is able to transport macromolecules with diameters of ~39 nm. *Mol. Biol. Cell*. **13**:425–434 (2002). Medline. doi:10.1091/mbc.01-06-0308.
42. R. Y. H. Lim, and B. Fahrenkrog. The nuclear pore complex up close. *Curr. Opin. Cell Biol*. **18**:342–347 (2006). Medline. doi:10.1016/j.ceb.2006.03.006.
43. C. -K. Chan, and D. A. Jans. Using nuclear targeting signals to enhance non-viral gene transfer. *Immunol. Cell Biol*. **80**:119–130 (2002). Medline. doi:10.1046/j.1440-1711.2002.01061.x.

44. I. A. Khalil, K. Kogure, H. Akita, and H. Harashima. Uptake pathways and subsequent intracellular trafficking in nonviral gene delivery. *Pharmacol. Rev.* **58**:32–45 (2006). Medline. doi:10.1124/pr.58.1.8.
45. H. Kamiya, H. Tsuchiya, J. Yamazaki, and H. Harashima. Intracellular trafficking and transgene expression of viral and non-viral gene vectors. *Adv. Drug Deliv. Rev.* **52**:153–164 (2001). Medline. doi:10.1016/S0169-409X(01)00216-2.
46. M. Colin, G. Maurice, G. Trugnan, M. Kornprobst, R. P. Harbottle, A. Knight, R. G. Cooper, A. D. Miller, J. Capeau, C. Coutelle, and M. C. Brahimi-Horn. Cell delivery, intracellular trafficking and expression of an integrin-mediated gene transfer vector in tracheal epithelial cells. *Gene Ther.* **7**:139–152 (2000). Medline. doi:10.1038/sj.gt.3301056.
47. J. Suh, D. Wirtz, and J. Hanes. Efficient active transport of gene nanocarriers to the cell nucleus. *Proc. Natl. Acad. Sci.* **100**:3878–3882 (2003). Medline. doi:10.1073/pnas.0636277 100.